Optoelectronic Devices Based on Mesomorphic, Highly Polarizable 1,3,5-Trisalkynyl Benzenes

Gunther Hennrich,*[,†] Emma Cavero,[§] Joaquín Barberá,[§] Berta Gómez-Lor,[‡] Robert E. Hanes,[||] Mara Talarico,[⊥] Attilio Golemme,[⊥] and José Luis Serrano*[,§]

Departamento de Química Orgánica, Universidad Autónoma de Madrid, and Insituto de Ciencia de Materiales de Madrid−CSIC, 28049 Madrid, Spain, Departamento de Química Orgánica, Facultad de Ciencias−ICMA, Universidad de Zaragoza−CSIC, 50009 Zaragoza, Spain, Beacon Sciences LLC, Austin, Texas, 78738, and Centro di Eccelenza CEMIF.CAL, INSTM UdR−Calabria, Dipartimento di Chimica, University of Calabria, 87036 Rende, Italy

Received September 13, 2007
Revised Manuscript Received October 11, 2007

The ability of discotic liquid crystals (LCs) to self-assemble into columnar stacks, enabling a one-dimensional transport of charge, makes them particularly suitable to be used as active layers in organic optoelectronic devices, such as light-emitting diodes (LEDs), photovoltaic cells (PVCs), and field-effect transistors (FETs).[1] In highly ordered discotic phases, high charge mobilities can be obtained[2] that are capable of surpassing the electronic properties of conventional polymeric materials. Such high-performance, electro-optical liquid-crystalline materials typically consist of large, polycyclic (hetero)aromatics,[3] whereas in contrast, low-molecular-weight benzene-based systems have not yet been reported as photoconductive materials, to the best of our knowledge. However, C_3-symmetric, π-expanded alkynylbenzenes are known to form columnar LCs and have been applied in electro-optical devices.[4]

Encouraged by our previous results on LC material for second-order nonlinear optics, here we whish to report new members of a family of discotic 1,3,5-trisalkynylbenzenes (**1**–**3**), their mesomorphic properties, and finally, the photoconductivity properties of the new LC materials. Compounds **1**–**3** are conveniently synthesized by 3-fold Sonogashira coupling of 1,3,5-triiodo-2,4,6-trisalcoxybenzene with the commercially available *p*-arylethynyl derivatives, in the same way as described for the preparation of **4** (Figure 1).[4c,5]

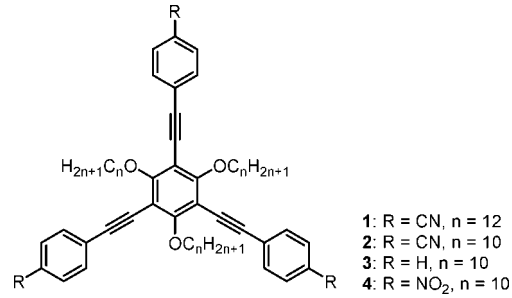

Figure 1. 1,3,5-Trisalkynylbenzene mesogens **1**–**4**.

As revealed by UV–vis and fluorescence spectroscopy in solution, the C_3-symmetric molecules **1**−**4** constitute highly polarizable π-systems of an octopolar donor−π-acceptor character with an electron-rich, alcoxy-substituted benzene core and an electron-deficient periphery. The effect on the electronic properties of **1**–**4** exerted by the terminal substituents is clearly reflected in their spectroscopic behavior: Increasing polarity resulting form the increasing electron-withdrawing capacity of the terminal *p*-phenyl substituents ($\sigma_p(H) = 0 < \sigma_p(CN) = 0.66 < \sigma_p(NO_2) = 0.78$)[6] is corroborated by bathochromic shifts of the absorption and emission spectra, accompanied by a general accentuation of the charge-transfer characteristics, marked by enhanced absorptivities, loss of vibronic structure, and large Stokes shifts.[7] Compounds **1**−**3** are well-fluorescent in solution with quantum yields Φ_{fl} between 0.42 (**1**, **2**) and 0.12 (**3**), respectively, whereas the nitro derivative **4** is virtually

* Corresponding author. E-mail: gunther.hennrich@uam.es.
† Departamento de Química Orgánica, Universidad Autónoma de Madrid.
§ Insituto de Ciencia de Materiales de Madrid−CSIC.
‡ Universidad de Zaragoza−CSIC.
|| Beacon Sciences LLC.
⊥ University of Calabria.

(1) (a) Sergeyev, S.; Pisula, W.; Geerts, Y. H. *Chem. Soc. Rev.* **2007**, *36*, 1902. (b) Adam, D.; Schuhmacher, P.; Simmerer, J.; Haussling, L.; Siemensmeyer, K.; Etzbach, K. H.; Ringsdorf, H.; Haarer, D. *Nature* **1994**, *371*, 141. (c) Kumar, S. *Curr. Sci.* **2002**, *82*, 256. (d) Levitsky, I. A.; Kishikawa, K.; Eichhorn, S. H.; Swager, T. M. *J. Am. Chem. Soc.* **2000**, *122*, 2474. (e) O'Neill, M.; Kelly, S. M. *Adv. Mater.* **2003**, *15*, 1135.

(2) Cohen, Y. S.; Xiao, S.; Steigerwald, M. L.; Nuckolls, C.; Kagan, C. R. *Nano Lett.* **2006**, *6*, 2838.

(3) (a) Kaafarani, B. R.; Kondo, T.; Yu, J.; Zhang, Q.; Dattilo, D.; Risko, C.; Jones, S. C.; Barlow, S.; Domercq, B.; Amy, F.; Kahn, A.; Brédas, J.-L.; Kippelen, B.; Marder, S. R. *J. Am. Chem. Soc.* **2005**, *127*, 16358. (b) Simpson, C. D.; Wu, J.; Watson, M. D.; Müllen, K. J. *Mater. Chem.* **2004**, *14*, 494.

(4) (a) Hsu, H.-F.; Lin, M.-C.; Lin, W.-C.; Lai, Y.-H.; Lin, S.-Y. *Chem. Mater.* **2003**, *15*, 2115. (b) Bushey, M. L.; Nguyen, T.-Q.; Nuckolls, C. *J. Am. Chem. Soc.* **2003**, *125*, 8264. (c) Hennrich, G.; Omenat, A.; Asselberghs, I.; Foerier, S.; Clays, K.; Verbiest, T.; Serrano, J. L. *Angew. Chem., Int. Ed.* **2006**, *45*, 4203.

(5) 1,3,5-Tris[4-(cyanophenyl)ethynyl]-2,4,6-tris(dodecyloxy)benzene (**1**). Pure **1** was obtained as off-white solid after final recrystallization from *i*-PrOH in 24% yield (121 mg). ^{1}H NMR (300 MHz, $CDCl_3$): δ 7.66 (d, J = 8.3 Hz, 6 H), 7.58 (d, J = 8.3 Hz, 6 H), 4.35 (t, J = 6.3 Hz, 6 H), 1.86 (q, J = 6.4 Hz, 6 H), 1.54 (q, J = 7.7 Hz, 6 H), 1.30–1.21 (m, 48 H), 0.88 (t,J = 9.9 Hz, 9 H). ^{13}C NMR (125 MHz, $CDCl_3$): δ 164.1, 132.1, 131.7, 128.1, 118.3, 111.7, 107.3, 95.6, 85.7, 75.2, 31.9, 30.5, 29.6(4), 29.6(0), 29.5(8), 29.4(8), 29.3, 29.2, 26.2, 22.6, 14.1. MALDI-MS *m*/*z* 1006 (M^+). Calcd for $C_{69}H_{87}O_3N_3$: C, 82.16; H, 8.65; N, 4.17. Found: C, 82.14; H, 8.88; N, 4.13. 1,3,5-Tris[4-(cyanophenyl)ethynyl]-2,4,6-tris(decyloxy)benzene (**2**). Pure **2** was obtained as an off-white solid after final recrystallization from *i*-PrOH in 18% yield (80 mg). ^{1}H NMR (300 MHz, $CDCl_3$): δ 7.66 (d, J = 8.2 Hz, 6 H), 7.58 (d, J = 8.2 Hz, 6 H), 4.35 (t, J = 6.3 Hz, 6 H), 1.86 (q, J = 6.3 Hz, 6 H), 1.54 (q, J = 7.4 Hz, 6 H), 1.31–1.26 (m, 36 H), 0.88 (t, J = 7.1 Hz, 9 H). ^{13}C NMR (125 MHz, $CDCl_3$): δ 164.1, 132.1, 131.7, 128.1, 118.4, 111.7, 107.3, 95.6, 85.7, 75.2, 31.9, 30.5, 29.6, 29.5(4), 29.5(0), 29.3, 26.3, 22.7, 14.1. MALDI-MS *m*/*z* 846 (M^+). Calcd for $C_{63}H_{75}O_3N_3$: C, 85.11; H, 9.22. Found: C, 84.81; H, 9.38.1,3,5-Tris(phenyl)ethynyl-2,4,6-tris(decyloxy)benzene (**3**). Pure **3** was obtained as waxy solid in 25% yield (107 mg). ^{1}H NMR (300 MHz, CDCl3): δ 7.56–7.53 (m, 6 H), 7.37–7.35 (m, 9 H), 4.37 (t, J = 6.2 Hz, 6 H), 1.90 (q, J = 6.3 Hz, 6 H), 1.59 (q, J = 7.5 Hz, 6 H), 1.32–1.22 (m, 36 H), 0.88 (t, J = 7.2 Hz, 9 H). ^{13}C NMR (125 MHz, CDCl3): δ 162.9, 131.3, 128.3, 128.2, 123.7, 108.3, 97.0, 81.6, 74.8, 31.9, 30.6, 29.6(3), 29.6(1), 29.5(8), 29.3, 26.3, 22.7, 14.1. MALDI-MS *m*/*z* 846 (M+). Calcd for $C_{60}H_{78}O_3$: C, 85.11; H, 9.22. Found: C, 84.81; H, 9.38.

(6) Hansch, C.; Leo, A.; Taft, R. W. *Chem. Rev.* **1991**, *91*, 165–195.

(7) Turro. N. J. *Modern Molecular Photochemistry*; University Science Books: Sausalito, CA, 1991.

10.1021/cm702617v CCC: $37.00
Published on Web 11/14/2007

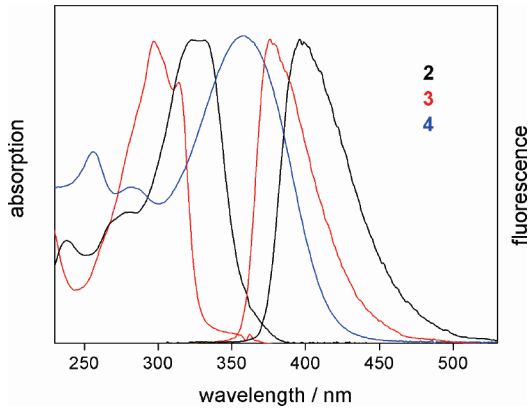

Figure 2. Normalized absorption and fluorescence (λ_{ex} = 300 nm) spectra of **2**–**4** in CH_2Cl_2; **1**, overlapping with **2**, omitted for clarity.

Table 1. Phase Behavior of 1–4

	Phase[a] T[b]/°C (ΔH / kJ mol^{-1})						
1	Cr	77	Col	83 (42.7)[c]	N_D	98 (0.4)	I
2	Cr	97 (38.8)	Col_r	128 (5.0)	N_D	134 (0.8)	I
3	Cr	42 (32.0)	I				
4	Cr	60	Col_h	69 (12.0)[c]	N_D	112 (0.7)	I

[a] Cr = crystal, I = isotropic liquid, Col_r = rectangular columnar, Col = columnar, Col_h = hexagonal columnar, N_D = discotic nematic. [b] DSC onset peaks. [c] Enthalpy sum of two transitions Cr−Col−N.

nonemissive (Figure 2). To probe the potential pratical use of the highly fluorescent cyano derivatives as active OLED material,[1e] we have studied the photoluminescence of **1** in the mesophase in a thick film sample, prepared by sandwiching the material at 100 °C between two silica substrates. Upon irradiation at 300 nm, the strong fluorescence is maintained in the solid state, registered as a featureless broad band centered around 422 nm, which is only a slight red shift compared to the solution experiment (see the Supporting Information, Figure S1). Furthermore, the computational calculation of the (second-order) polarizability β for the octopolar compounds **2**−**4** verifies the tendencies observed by linear optical spectroscopy. The matrix elements in x and y planes contribute significantly to the β-value, whereas the components in the z direction, perpendicular to the molecule plane, can be neglected (see the Supporting Information). As discussed below, the comparison of spectroscopic and mesomorphic propierties points to an elevated polarizability of the π-systems as a requierement for mesomorphism.

As expected from the previous results obtained for the nitro analogues, cyano derivatives **1** and **2** also exhibit liquid crystal properties with discotic mesophases, which have been characterized using polarized light optical microscopy (POM), differential scanning calorimetry (DSC), and powder X-ray diffraction (XRD). In contrast, **3** forms an anisotropic melt upon heating without the intermediate presence of a LC mesophase. Transition temperatures and their associated enthalpy changes are summarized in Table 1.

Both compounds show columnar and discotic nematic mesophases. However, the increase in the chain length in two carbon atoms destabilizes the mesomorphism and reduces the transition temperatures. The discotic nematic mesophases have

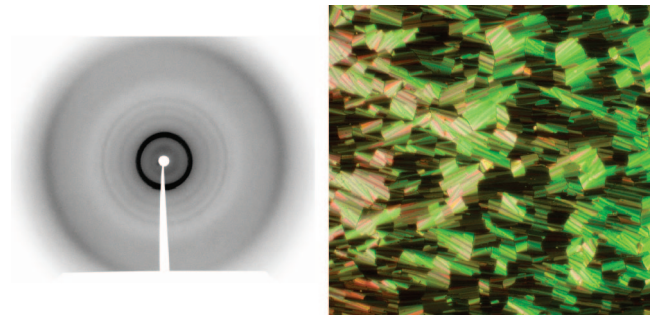

Figure 3. Powder XRD pattern of **2** in the Col_r phase (left) and POM image of **2**at 122 °C (right).

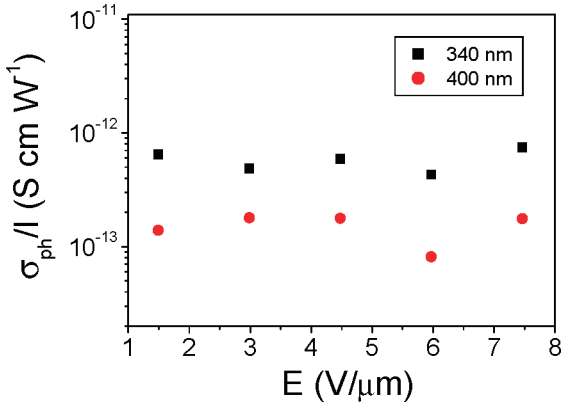

Figure 4. Photoconductivity of **1** as a function of the applied electric field. As the photoconductivity depends on light intensity, experimental data are normalized to the light power density I.

been identified by their typical droplet schlieren textures observed by POM. The columnar ones exhibit fan-shaped like textures for compound **2** (Figure 3) and mosaic textures for **1** (see the Supporting Information, Figure S2), characteristic of columnar mesophases. Further studies by XRD have allowed us to determine the symmetry of the columnar arrangement of **2**. The XRD pattern obtained for the compound was consistent with a rectangular columnar phase (Col_r). This mesophase was identified by the presence of a set of low-angle maxima related to a two-dimensional array of columns with a lattice parameters a = 32 Å and b = 21.4 Å. An additional halo appears at high angles, corresponding to the average stacking distance of the mesogenic cores of 4.2 Å. The density calculated for this mesophase is 1.06 g cm^{-3}, on the basis of two molecules per unit cell (Z = 2), as occurs for most of the rectangular columnar mesophases. This means that the rectangular lattice contains one column at the center and one molecule at the corner of the rectangle. Unfortunately, because of the narrow range of the columnar mesophase, for **1**, it was not possible to obtain good XRD patterns in the mesophase to permit us to assign it as a rectangular or hexagonal columnar phase; nevertheless, mosaic textures are usually associated to hexagonal ones. When comparing nitro and cyano derivatives, the higher tendency of cyano derivatives to arrange in columns is worth noting. Such columnar mesophases appear in wider thermal ranges and exhibit a higher degree of order. This has led us to explore the features of these compounds as photoconductors.

Figure 4 shows the applied-electric-field dependence of the photoconductivity measurement of a 7 μm thick sample of **1** under illumination with unpolarized light at two different

wavelengths, 340 and 400 nm. The higher values of σ_{ph}/I as a function of E were obtained by irradiating the sample with light at 340 nm ($\sigma_{ph}/I = 7.4 \times 10^{-13}$ S cm W^{1-} with an applied field $E = 7.5$ V μm^{-1}). As photoconduction is not very high, its usual applied field dependence is not evident from the data and is probably hidden by the experimental error. At 200 and 500 nm, no photoconduction was detected. The wavelength dependence of σ_{ph}/I is consistent with the absorption spectrum of the material. To check this point, we measured the absorption coefficient α of **1** at the same wavelengths at which photoconduction measurements were performed, as shown in Figure 5, where values of σ_{ph}/I at $E = 7.5$ V/μm are also indicated.

The higher the absorption, the higher the photoconduction; for low absorption, no photoconduction could be detected. Compound **1** shows modest photoconductivity, but only for wavelengths close to the absorption maximum (Figure 5).

In conclusion, new liquid-crystalline materials based on structurally simple, low-molecular-weight mesogens have been prepared and characterized by optical spectroscopy on the molecular level and by POM, DSC, and XRD for the liquid crystal phase. Apart from a first indication of efficient photoluminescence of **1** in the bulk phase, photoconductivity

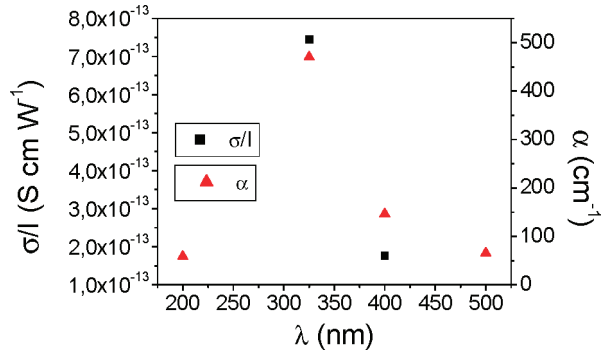

Figure 5. Normalized photoconductivity (squares) and absorption coefficient(triangles) of **1** at different wavelengths.

of **1** in the bulk material is modest. Nonetheless, it should be considered that the absorption coefficient is also low and that measurements were performed on the pure material, without adding any photosensitizer to boost charge generation. A promising strategy to overcome the relatively large intercore distances between the discotic mesogens, potentially the main reason for the low photoconductivity, is to enhance the attractive interactions between discotic molecules via the introduction of functional groups to enforce intermolecular hydrogen-bonding.[9] Efforts in this direction are underway.

Acknowledgment. This work was supported by the MEC (Spain) and FEDER (EU) funds (Projects CTQ2004-02865_BQO, MAT 2006-013571-CO2, CTQ 2006-15611-CO201), and by MIUR under the Project Molecular and Organic/Inorganic Hybrid Nanostructure for Photonics—FIRB 2001.

Supporting Information Available: Fluorescence spectra of **1**; POM images of **1** and **2**; theoretical calculations; experimental details (PDF). This material is available free of charge via the Internet at http://pubs.acs.org.

CM702617V

(8) The photoconductive properties of **2** were characterized at room temperature on samples sandwiched between two clean ITO covered glass slides without any surface treatment. The plates were assembled into cells using 7 μm spacers to control the thickness and a bicomponent UV-cured epoxy as a sealant. The thickness of the empty cells was checked by interferometric mesurements. Cells were filled by capillarity with **2** in the isotropic phase (at 110°C) and then cooled rapidly to room temperature, in the crystalline phase. Observation of the prepared samples at the polarizing microscope confirmed the presence of randomly oriented crystalline domains. Photoconductivity of **2** was determined by applying a DC electric field and then measuring the current flowing through the cell, with and without light exposure, with a Keithley 6517A electrometer. Because photogeneration depends on the light power density I, results are presented in terms of the σ_{ph}/I ratio. Measurements were performed at 4 different wavelengths (200, 340, 400, and 500 nm) of the incident light as a function of the applied electric field. A 300 W xenon lamp (LOT Oriel) was used as a light source, and the desired wavelength was selected by a motorized monochromator (Oriel Instruments, CornerstoneTM 260 1–4 M, model 74100). The actual power of the radiation incident on the sample was measured using a power meter (UV Silicon Probe 70282 LOT Oriel).

(9) Gearba, R. I.; Lehmann, M.; Levin, J.; Ivanov, D. A.; Koch, M. H. J.; Barberá, J.; Debije, M. G.; Piris, J.; Geerts, Y. H. *Adv. Mater.* **2003**, *15*, 1614.